Research Article

Dong Li, Yuhang Pan, Changjiang Liu*, Peiyuan Chen, Yuyou Wu, Jian Liu, Zhoulian Zheng, and Guangyi Ma

Optimal design of glazed hollow bead thermal insulation mortar containing fly ash and slag based on response surface methodology

https://doi.org/10.1515/rams-2022-0313 received November 05, 2022; accepted April 24, 2023

Abstract: Fly ash (FA) and slag could improve the performance of glazed hollow bead (GHB) thermal insulation mortar, but little research touched on how the FA and slag affect its performance and optimize its component contents. In this study, an experimental and statistical investigation is conducted to analyze the influences of FA and slag variables on the performance of GHB mortar based on the response surface methodology (RSM). The predicted model was proved statistically significant in terms of the fluidity, compressive strength, flexural strength, and thermal conductivity. Then, the validated model was used to identify the critical parameters and discuss their mechanisms of action. It can be found that (i) FA plays a significant role in fluidity and compressive and flexural strength owing to its morphological and physical filler effects; (ii) slag has an obvious influence on compressive strength and thermal conductivity due to its microaggregate effect. Finally, optimization design was conducted using the desirability approach of RSM to give the optimal component of 20.73% FA and 21.49% slag. The predicted combination was validated by confirmatory tests within an error of 1.52%. This study provides a feasible and effective solution for optimizing GHB thermal insulation mortar to achieve higher performance.

Dong Li, Peiyuan Chen: School of Human Settlements and Environments, Quanzhou Vocational and Technical University, Quanzhou 362268, China

Yuhang Pan, Jian Liu, Guangyi Ma: School of Civil Engineering, Guangzhou University, Guangzhou 510006, China Yuyou Wu: School of Transportation, Civil Engineering and Architecture, Foshan University, Foshan, Guangdong 528000, China Zhoulian Zheng: School of Civil Engineering, Chongqing University, Chongqing 400044, China

Keywords: glazed hollow bead mortar, fly ash, slag, optimization, response surface methodology, thermal insulation material

1 Introduction

Due to the rapid development of building construction, there exist a large amount of energy and resource consumption, which has induced environmental problems. It is reported that the energy dissipation through the building walls can reach over 60% of the total energy dissipation of buildings [1]. Therefore, developing thermal insulation in building is an efficient method to realize the global energy conservation of buildings and the sustainable development of the construction industry [2,3]. Thermal insulation material plays a critical role in designing and constructing energy-saving buildings.

In recent decades, dozens of thermal insulation materials with a large number of closed pores inside have been developed and applied, such as ceramsite mortar [4], foam mortar [5], aerated mortar [6], and slag mortar [7]. Due to the unique pore structure, the thermal insulation mortar has a low thermal conductivity and excellent thermal insulation. Among them, the glazed hollow bead (GHB) mortar has attracted much attention due to its better thermal insulation performance, satisfied fire prevention, and mechanical characteristics [8–10]. The GHB embedded in mortars acts as hollow sand and a "solid air-entraining agent" for the construction material [11]. However, the application of GHB mortars may reduce the compressive strength and skid resistance owing to their loose porous structure inside, which has a negative impact on building safety [12]. Furthermore, the fresh GHB mortar could be considered a solid-liquid two-phase mixture, and it may become susceptible to segregation, bleeding, or a lack of fluidity if not properly proportioned. When the fluidity and uniformity are poor, the pipe is prone

^{*} Corresponding author: Changjiang Liu, School of Civil Engineering, Guangzhou University, Guangzhou 510006, China, e-mail: cjliu@gzhu.edu.cn

to being plugged, reducing engineering efficiency and increasing the project cost [13].

Due to the positive effects of fly ash (FA) and slag on the various properties of mortar, including workability, strength, and durability, the FA and slag originating from industrial and municipal solid waste can be utilized as additional binder compositions. In addition to the improvements in properties, the partial replacement of cement using FA and slag can address issues in carbon dioxide emissions, waste recycling, and energy and resource consumption, which would realize the sustainability of the construction industry. Some investigations have been carried out on the effect of FA and slag on the performance of GHB mortar. Fan and Wang [14] identified the effects of FA with different contents on the long-term drying shrinkage of GHB mortar. It can be obtained that the drying shrinkage of GHB mortar reduced by more than 20 with 54% FA, compared with the blank group. Zaibo et al. [15] concluded that with FA content increasing by 10%, both fluidity and compressive strength of GHB mortar decreased by 10.6 and 13.8%, respectively. Wan et al. [16] found that the thermal conductivity of the thermal insulation system increased by 16.17% with 30% iron slag. It can be concluded that iron slag may be applied as a component of thermal backfill materials to improve the thermal conductivity. Ghosh et al. [17] identified the overall heat transfer co-efficient of thermal insulation wall panel with 50% FA reduced by 15.58%, compared with the blank group. Wang et al. [18] applied the FA to produce a C40 strength-class GHB concrete while maintaining the thermal conductivity of 0.45 W·m⁻¹·K⁻¹. He and Liu [19] found that FA can reduce the drying shrinkage of the GHB mortar owing to the water loss of the mortar and the pore structure of the cement paste based on the capillary force theory. Furthermore, Maria and Hamlin [20] revealed that the relationship between the gel pore with a radius less than 4 nm and the drying shrinkage showed a linear growing trend.

According to previous studies, it has been demonstrated that both FA and slag can improve the properties of GHB thermal insulation mortars, such as fluidity, strength, drying shrinkage, and thermal conductivity. Among them, it is mainly focused on the individual contribution of one component, either FA or slag, to the material properties. Until now, it has been hard to find relevant literature reporting the simultaneous action of FA and slag components on the performance of GHB mortars comprehensively. In fact, there exist interactions between various components that affect the fluidity, strength, and thermal conductivity of GHB mortars. Little research has been conducted to establish the correlation between components and performances and further optimize the formulation of GHB mortars containing FA and slag.

To address the deficiency, the originality of this study is to optimize the GHB thermal insulation mortars containing FA and slag that can balance the fluidity, strength, and thermal conductivity and finally give the optimal dosing range of each component. Two optimized parameters including FA and slag contents are selected. Then, the effects of these parameters on the fluidity, strength, and thermal conductivity of GHB mortars are investigated individually and interactively. In order to identify the optimum parameters, an optimization investigation is carried out using the response surface methodology (RSM) by maximizing the fluid and strength while minimizing the thermal conductivity. The study would provide optimal component contents about the feasibility of incorporating FA and slag as potential cementitious materials in the thermal insulation materials.

2 Materials and experiments

2.1 Materials

Ordinary Portland cement PO 42.5, class II FA, and granulated blast furnace slag were employed as the mineral additions in the experiment. The chemical compositions of cement, FA, and slag are listed in Table 1. GHB is an irregular sphere of granules, as shown in Figure 1. The performance indicators are shown in Table 2. The particle size distributions of cementitious materials and GHB are shown in Figure 2. Polycarboxylate superplasticizer (PCE) was used to improve the fluidity of the fresh mortar. Redispersible polymer powder (RDP), hydroxypropyl methylcellulose (HPMC), tartaric acid retarder (TAR), and defoaming agent were used as chemical additive agencies in the experiment.

2.2 Formulation design

RSM is a collection of mathematical and statistical techniques that allow multiple responses to be set for each

Table 1: Chemical compositions of cement, FA, and slag, wt%

	CaO	SiO ₂	Al ₂ O ₃	Fe ₂ O ₃	Mg0	SO ₃	R ₂ O
Cement	61.02	20.94	4.85	3.44	3.22	2.32	0.5
FA	4.01	52.97	33.15	4.16	1.01	1.5	2.04
Slag	40	42	16	0.57	0.41	0.51	0.23



Figure 1: A photograph of GHB samples.

control variable. After all the responses are established, the best response value (i.e., optimal component contents) can be identified from the response surface or contour plot [21]. In this study, two factors, including FA and slag contents (i.e., X_1 and X_2), are needed to be optimized, and the test cases are typical, representing the extreme conditions. Thus, the central composite design method in RSM is applied to evaluate the effects of the FA and slag contents on multiple responses. Then, a series of 13 twovariable, five-level experiments were carried out. The surface response tests are designed through the Design-Expert version 12.0.6 software to identify the optimized content of the FA and slag components. The level and coding of the design are shown in Table 3. The FA is a continuous variable of 10-40%, and the slag is a continuous variable of 10–40%. The distance α of the axial runs from the design center and can be calculated depending on the number of points $(n_{\rm F}=2^k)$, where k is the number of variables (k = 2). Consequently, α can be obtained as $\alpha =$ $(n_{\rm E})^{1/4}$ = 1.41. The additives including PCE, HPMC, TAR, and defoaming agent are not considered as variables, and their contents are 0.86, 0.18, 0.1, and 0.2%, respectively.

The design matrix of the 13-point optimal experiment is carried out, and the detailed experimental design is shown in Table 4. Each design is evaluated independently to investigate the influence of each variable on the responses. In order to reduce and expand the representativeness of the test, the duplicated points are set as

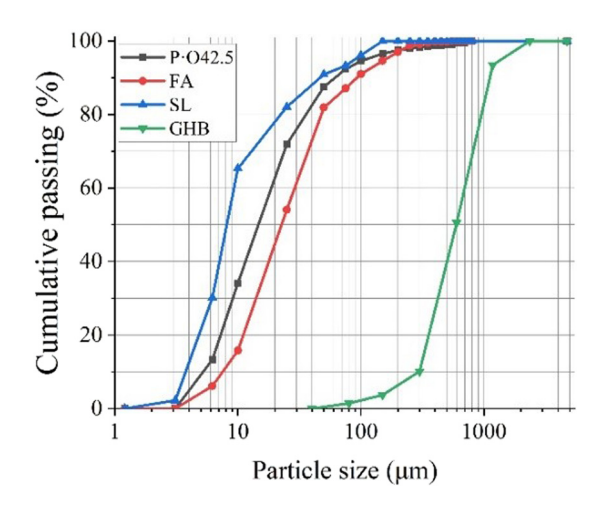


Figure 2: The particle size distribution of powders and GHBs.

Table 3: Level and coding of the design of FA and slag variables

Experimental	Symbol		Coded levels and values				
variable		-α -1.41	Low -1	0 0	High 1	+α 1.41	
FA (%) Slag (%)	X ₁ X ₂	3.79 3.79	10 10	25 25	40 40	46.21 46.21	

shown in Table 4. Finally, response variables including fluidity, compressive strength, flexural strength, and thermal conductivity can be identified after tests.

2.3 Preparation process

Figure 3 illustrates the preparation process of GHB mortar. First, the PCE was added into water and mixed by the LC-OES-60 cantilever electric mixer at 1,200 rpm for 2 min. Then, the mixture, including PO 42.5, FA, slag, and GHB, is weighted and put into the UJZ-15 mortar mixer. Subsequently, the LC-OES-60 cantilever electric mixer is used to mix at 1,000 rpm for 1 min. Finally, the water with PCE, mixture, and additives are added to the container and mixed at 500 rpm for 3 min to obtain the GHB mortar.

Table 2: Technical indicators of GHBs

Items	Density (kg·m ⁻³)	Compressive strength (kPa)	Thermal conductivity (W·m ⁻¹ ·K ⁻¹)	Obturator rate of vitrified surface (%)	Floating rate (%)
Results	103	187	0.042	95	93

Table 4: Experimenta	l design for the	formulation of	of GHB mortar
----------------------	------------------	----------------	---------------

Run	Cement (%)	Water (%)	GHB (%)	RDP (%)	FA (%)	Slag (%)
1	100	50	30.76	2	25	25
2	100	50	30.76	2	25	3.79
3	100	50	30.76	2	25	25
4	100	50	30.76	2	40	10
5	100	50	30.76	2	25	25
6	100	50	30.76	2	10	40
7	100	50	30.76	2	25	46.21
8	100	50	30.76	2	25	25
9	100	50	30.76	2	46.21	25
10	100	50	30.76	2	40	40
11	100	50	30.76	2	3.79	25
12	100	50	30.76	2	10	10
13	100	50	30.76	2	25	25

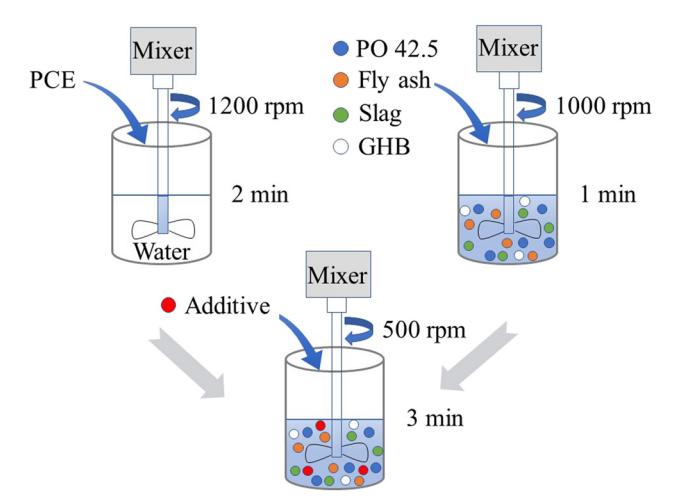


Figure 3: The GHB mortar preparation procedure.

3 Test methods

Fluidity, compressive strength, flexural strength, and thermal conductivity are all critical properties that are needed to be balanced and regarded as response variables during the optimal design process. The tests of the properties are conducted according to the Chinese standards.

3.1 Fluidity test

The flow diameter of GHB mortar is served as the critical parameter of fluidity and tested according to the Chinese Standard JGJ/T70-2009 [22]. The flow diameter of GHB mortar is measured by a glass plate and a hollow metal cylinder with an inner diameter of 30 mm and a height of 50 mm. First, the metal cylinder is placed at the center of

the glass plate. After filling the metal cylinder with GHB mortar, as shown in Figure 4(a), the metal cylinder is vertically raised sharply beyond 50 mm. Then, the mortar remains free-flowing for 15 s. Finally, the diameter of GHB mortar in two orthogonal directions is identified by rulers as shown in Figure 4(b).

3.2 Strength test

The 28-day compressive and flexural strengths of GHB mortar were studied following the Chinese Standard GB/T 17671-2021 [23]. Specimens for compressive strength tests were cast in three prismatic samples of 70.7 mm \times 70.7 mm, while those for flexural strength tests were cast in samples of 40 mm \times 40 mm \times 160 mm. Then, the specimens were cured for 28 days at a temperature of 20°C and a humidity of 95% in standard cure chambers. The specimens were tested by the electronic universal testing machine to obtain their compressive and flexural strengths, as shown in Figure 5.

3.3 Thermal conductivity test

The thermal conductivity of GHB-mortar is tested based on the Chinese Standard GB/T 32981-2016 [24]. Specimens were cast in 70 mm \times 70 mm \times 20 mm and cured for 3 days in standard cure chambers. Then, the cured specimens were dried for 25 days at 105°C in curing ovens. The thermal conductivity of specimens was measured by the Sweden Hot Disk 2500S thermal conductivity analyzer, as shown in Figure 6.





Figure 4: A fluidity test device (a) and its testing process (b).





Figure 5: A strength test device and its testing process: (a) compressive test and (b) flexural test.





Figure 6: Thermal conductivity and its testing process: (a) thermal conductivity analyzer and (b) thermal conductivity test.

6 — Dong Li et al. DE GRUYTER

Table 5: The experimental results of fluidity, strength, and thermal conductivity of specimens

Runs	Fluidity, Y ₁ (mm)	Compressive strength, Y ₂ (MPa)	Flexural strength, Y ₃ (MPa)	Thermal conductivity, Y ₄ (W·m ⁻¹ ·K ⁻¹)
1	124.5	22.52	4.7	0.67
2	123.5	20.83	4.57	0.68
3	125.0	22.92	4.67	0.67
4	119.0	20.07	4.20	0.68
5	121.5	23.12	4.77	0.67
6	114.0	22.05	5.03	0.70
7	126.0	19.93	4.63	0.70
8	125.5	22.85	4.83	0.67
9	117.5	18.41	4.13	0.67
10	122.0	18.35	4.17	0.68
11	107.0	22.72	5.16	0.67
12	112.5	21.46	4.87	0.67
13	122.0	22.84	4.73	0.66

4 Results and discussions

Table 5 summarizes the properties of each test formulation, including fluidity (Y_1) , compressive strength (Y_2) , flexural strength (Y_3) , and thermal conductivity (Y_4) . In addition, the analysis of variance (ANOVA) results of the fitted models for each case are presented in Table 6. The comparison between predicted and actual values is illustrated in Figure 7. The influences of variables including FA (X_1) and slag (X_2) on the response variables $(Y_1 - Y_4)$ will be discussed further.

4.1 Properties

4.1.1 Fluidity

The flow diameter of GHB mortar specimens is listed in Table 5. The ANOVA is performed to evaluate the significance of the fitted model in Table 6. The results of R^2 and Adj- R^2 are 0.95 and 0.92, respectively, which indicates a relative high degree of correlation between predicted and actual values. The Adeq-precision means the signal-to-

noise ratio, and its value of 17.20 is much larger than 4, which suggests an adequate signal without the significant effects of noise. The F-value of the model is 28.71, and the p-value is only 0.0002, indicating the efficiency of the fluidity regression model. These ANOVA results prove the accuracy of the predicted model using RSM. The predicted polynomial fitting equation for the flow diameter is as follows:

$$Y_1 = 81.37 + 298.76X_1 - 4.14X_2 - 33.33X_1X_2 - 545X_1^2 + 10.56X_2^2.$$
 (1)

Table 7 presents the significance of FA and slag on the fluidity of the GHB mortar. The *p*-value less than 0.05 indicated that the model terms were significant. In this case, the significant model terms are X_1^2 and X_1 in order of importance, which means that FA has a significant impact on the fluidity while slag has a slight influence. As shown in Figure 8, with the increase in FA content, the fluidity of mortar shows an obvious increase first within 30% FA content. The phenomena may be due to the "morphological effect" of FA and slag. Due to the smooth surface of spherical particles, FA filler added into mortars can diminish internal friction resistance, reduce water, and increase fluidity. However, the shape of slag particles appears irregular and polygonal, which has a negative impact on fluidity [25]. Another reason is that both FA and slag can result in a "micro-aggregate effect." The proper contents of FA, slag, and PO 42.5 may promote a reasonable microaggregate gradation and further improve the pore structure of GHB mortars [26]. However, there is a decreasing trend in fluidity with the content of FA over 30%, which is associated with the bleeding of mortars. Part of the mortar is separated from the GHBs aggregate, which leads to a reduction in fluidity.

4.1.2 Strength

According to the ANOVA results listed in Table 6, R^2 of compressive and flexural strength are 0.99 and 0.98, respectively, while the corresponding $Adj-R^2$ are 0.98

Table 6: The ANOVA results of the fitted models for each response variable

Response	R ²	Adj- <i>R</i> ²	Pred-R ²	Adeq-precision	<i>F</i> -value	<i>p-</i> Value
<i>Y</i> ₁	0.95	0.92	0.85	17.20	28.71	0.0002
Y_2	0.99	0.98	0.97	32.21	155.34	< 0.0001
<i>Y</i> ₃	0.98	0.97	0.94	27.37	74.19	< 0.0001
Y_4	0.96	0.92	0.85	15.54	28.77	0.0002

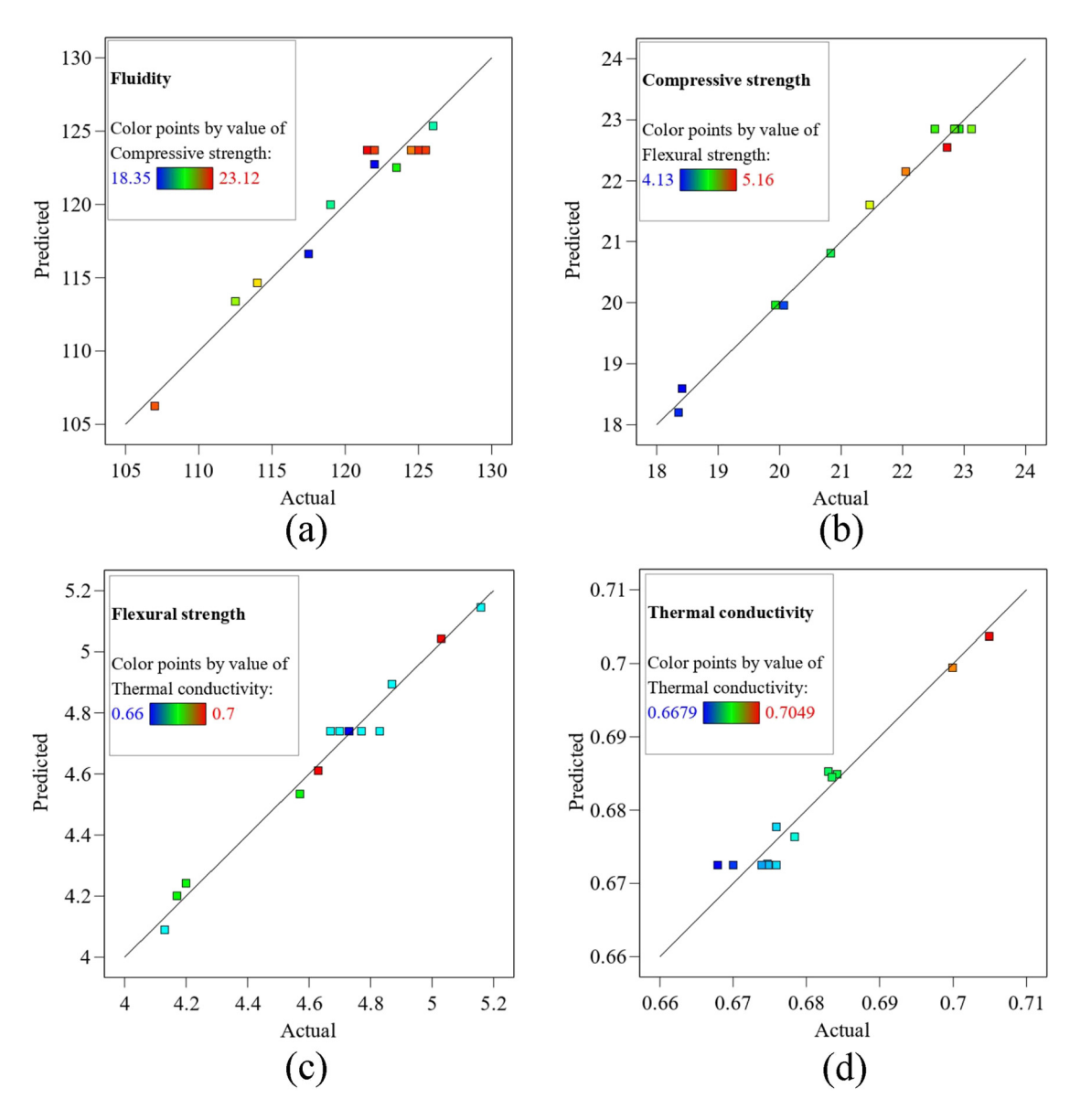


Figure 7: A comparison of predicted values of property indexes with actual test results: (a) fluidity, (b) compressive strength, (c) flexural strength, and (d) thermal conductivity.

Table 7: The ANOVA results of the fitted models for fluidity

Source	Degrees of freedom	<i>F</i> -value	<i>p</i> -Value	Significant
Model	5	28.71	0.0002	Yes
X_1	1	40.28	0.0004	Yes
X_2	1	3.02	0.1258	No
X_1X_2	1	0.2104	0.6603	No
X_1^2	1	97.83	<0.0001	Yes
X_2^2	1	0.0367	0.8535	No
Lack of fit	3	0.5426	0.6786	No

and 0.97, respectively. It is suggested that the predicted values in fitted models can be highly correlated with actual values of strength in test. The Adeq-precision of compressive and flexural strength are 32.21 and 27.37, respectively. Correspondingly, the F-values are 155.34 and 74.19, respectively. The p-values of these parameters are less than 0.0001, which indicates the accuracy of the strength regression model. The polynomial fitting equation of the 28-day compressive strength model is as follows:

$$Y_2 = 10.46 + 50.32X_1 + 64.78X_2 - 51.33X_1X_2 - 101.33X_1^2 - 109.56X_2^2.$$
 (2)

8 — Dong Li et al. DE GRUYTER

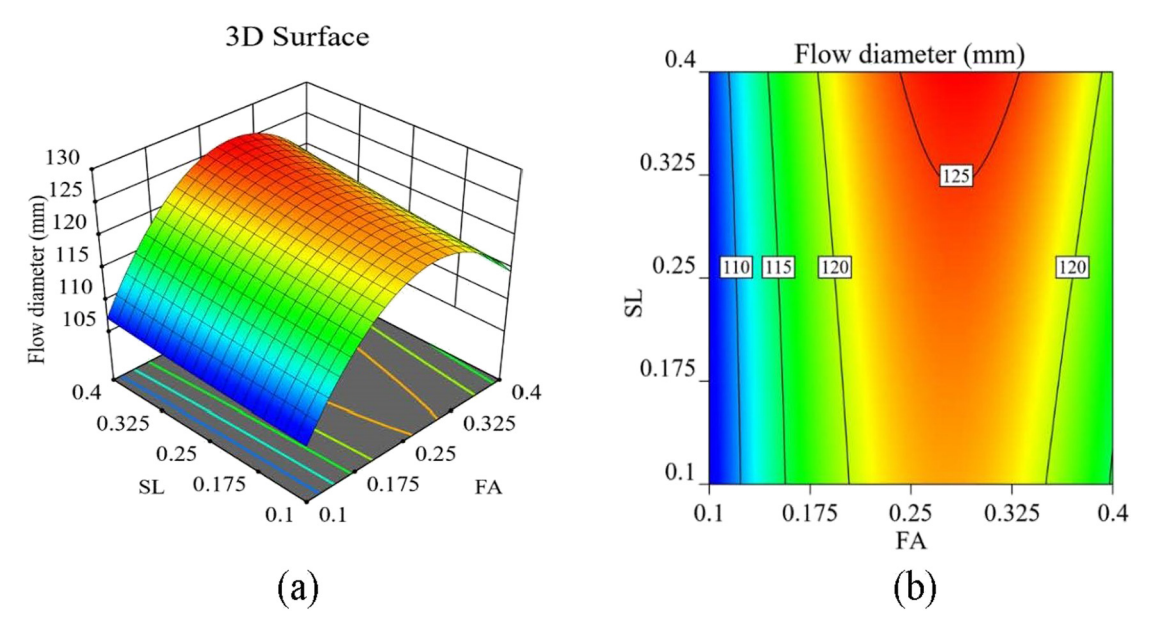


Figure 8: The influence of components on the fluidity of GHB mortar: (a) 3D plot and (b) contour plot.

Table 8 presents the significance of FA and slag on the flexural strength of the GHB mortar. The significant model terms can be identified as X_1 , X_1^2 , X_2^2 , X_1X_2 , and X_2 in order of importance, which means that both FA and slag have a significant influence on fluidity. With the increase of FA and slag, the compressive strength of mortar increases first and then decreases gradually, as shown in Figure 9. There is a maximum compressive strength at the point of 20% FA and 25% slag. The increasing trend in compressive strength may be associated with the "physical filler effect." The higher fineness of FA and slag can provide a physical filling effect to improve the compactness and compressive strength of GHB mortar, together with the amount of crystal phase Ca(OH)₂ and harmful pour reduction [27]. However, the incorporation of a large amount of FA and slag may

reduce the reactive GHB content and result in a reduction in compressive strength.

Furthermore, the polynomial fitting equation of the 28-day flexural strength can be obtained as follows:

$$Y_3 = 4.49 + 0.26X_1 + 5.03X_2 - 4.22X_1X_2 - 5.44X_1^2$$

$$- 7.44X_2^2.$$
 (3)

Based on the ANOVA results for flexural strength, the significant model terms can be identified as X_1 , X_2^2 , and X_1^2 in order of importance. It can be found that FA exhibits a dominant role in the 28-day flexural strength of GHB mortar. Since the pozzolanic reaction between FA and cement lags behind cement hydration, the GHB mortar strength at early curing age performs poorly and decreases with increasing FA content, as shown in Figure 10. When FA content is fairly high, cement is remarkably diluted,

Table 8: The ANOVA results of the fitted models for compressive and flexural strength

Source		Compressive strength			Flexural strength		
	F-value	<i>p</i> -Value	Significant	F-value	<i>p-</i> Value	Significant	
Model	155.34	<0.0001	Yes	74.19	<0.0001	Yes	
<i>X</i> ₁	346.57	< 0.0001	Yes	345.70	< 0.0001	Yes	
X_2	15.99	0.0052	Yes	1.79	0.2229	No	
X_1X_2	29.56	0.0010	Yes	2.80	0.1383	No	
X ₁ ²	200.35	<0.0001	Yes	8.09	0.0249	Yes	
X_2^2	234.19	<0.0001	Yes	15.13	0.0060	Yes	
Lack of fit	0.9213	0.5071	No	0.5964	0.6501	No	

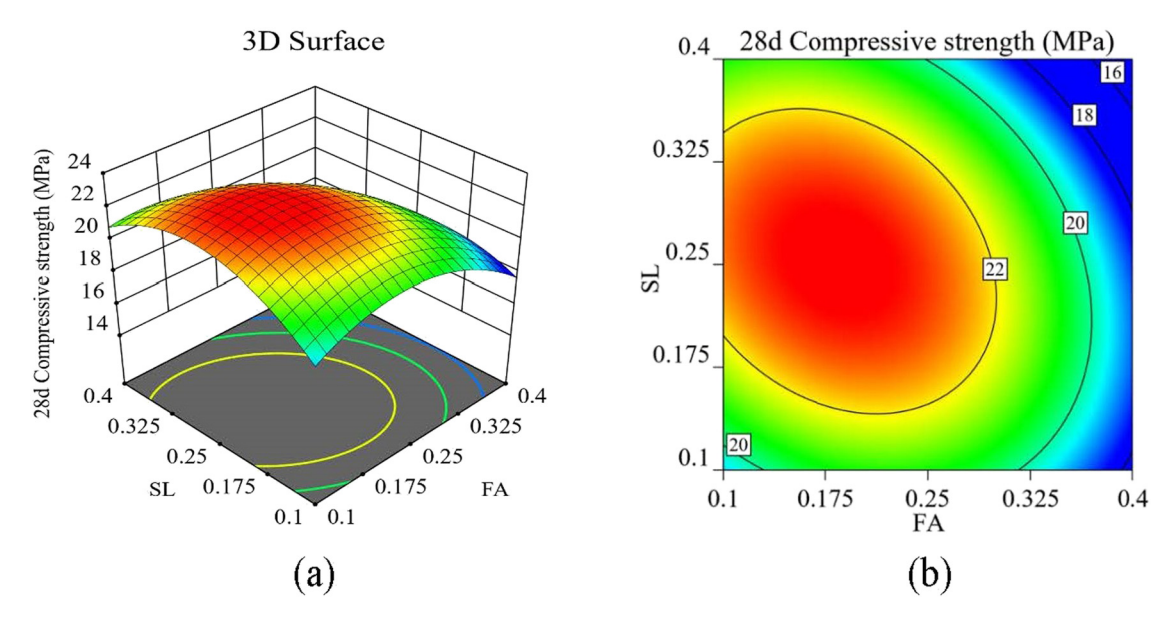


Figure 9: The influence of components on the compressive strength of GHB mortar: (a) 3D plot and (b) contour plot.

resulting in little hydration product in the GHB mortar and being unable to provide sufficient flexural strength. Therefore, the "diluting action" of FA at an early curing age contributes to the adverse effects of FA [28].

However, the slag content-flexural strength curve shows an increasing trend, as shown in Figure 10. The phenomenon is attributed to the "physical filler effect" that the compactness and flexural strength of GHB mortar would be enhanced due to the gaps between cement particles filled by finer slag particles. Another reason is that the slag could promote the hydration reaction and reduce

the calcium ion concentration between cement and coarse aggregates. Thus, the flexural strength of GHB mortar was improved after the addition of slag.

4.1.3 Thermal conductivity

Based on the ANOVA results listed in Table 6, R^2 and Adj- R^2 in the predicted thermal conductivity model are 0.96 and 0.92, respectively, which indicates that the model is statistically significant. The Adeq-precisions and F-values

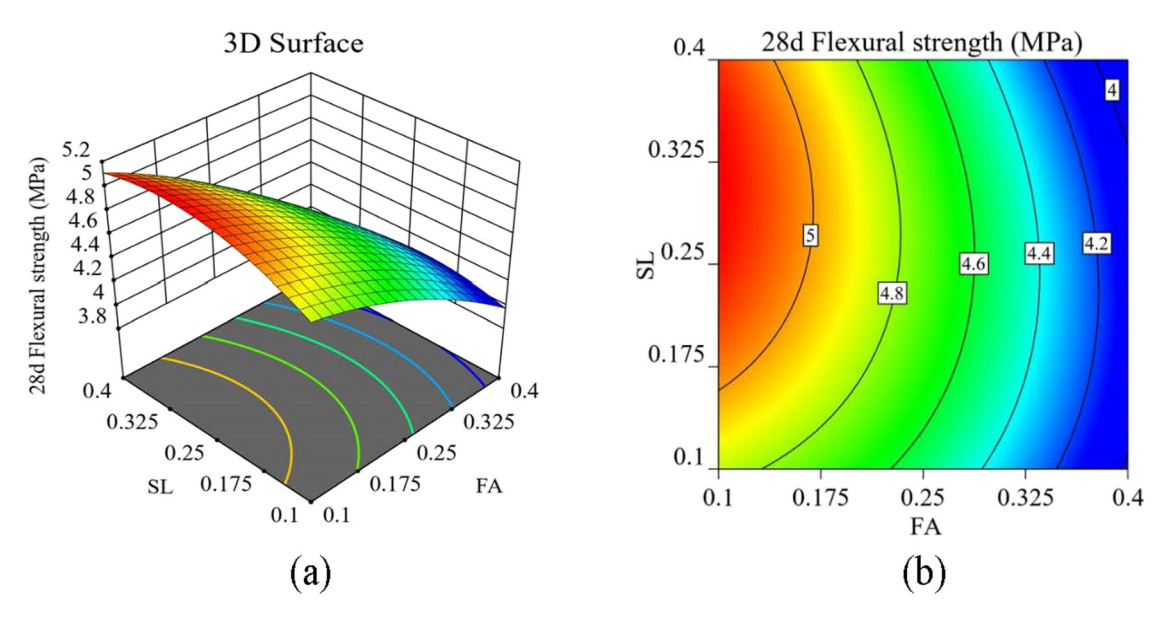


Figure 10: The influence of components on the flexural strength of GHB mortar: (a) 3D plot and (b) contour plot.

10 — Dong Li et al. DE GRUYTER

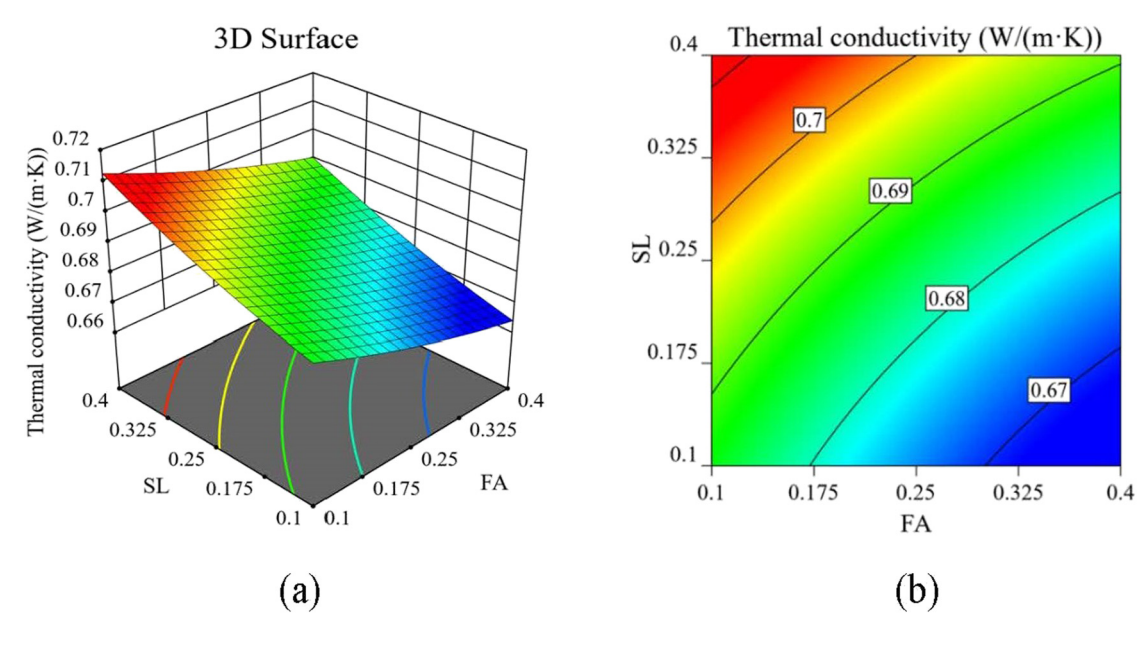


Figure 11: The influence of components on the fluidity of GHB mortar: (a) 3D plot and (b) contour plot.

Table 9: The ANOVA results of the fitted models for thermal conductivity

Source	Degrees of freedom	<i>F</i> -value	<i>p-</i> Value	Significant
Model	5	28.77	0.0002	Yes
X_1	1	0.1975	0.6702	No
X_2	1	38.94	0.0004	Yes
X_1X_2	1	18.43	0.0036	Yes
X_1^2	1	3.79	0.0927	No
X_2^2	1	85.73	< 0.0001	Yes
Lack of fit	3	0.5736	0.6609	No

are sufficiently high, with values of 15.54 and 29.97, respectively. The p-value is 0.0002 and much less than 0.05, which indicates that the thermal conductivity regression

model is desirable. The polynomial fitting equation of the thermal conductivity model is as follows:

$$Y_4 = 0.69 + 0.06X_1 - 0.25X_2 - 0.59X_1X_2 + 0.15X_1^2 + 0.91X_2^2.$$
(4)

As suggested in the ANOVA results for thermal conductivity, the significant model terms can be obtained as X_2^2 , X_2 , and X_1X_2 in order of importance. As shown in Figure 11, it can be found that slag exhibits a critical role in the thermal conductivity of GHB mortar rather than FA. Similar to a resistor in an electric field, GHB with a low thermal conductivity performs as a "thermal resistor." Due to the presence of GHB and fillers, the large heat flow channel in the mortar is continuously cut off and compressed, ultimately reducing the overall heat transfer capacity and thermal conductivity. The reason

Table 10: Optimization criteria for the factors and responses

Factors and responses	Target	Lower limit	Upper limit	Importance
FA (%)	In range	10	40	++
Slag (%)	In range	10	40	++
Fluidity (mm)	Maximize	107	126	+++
Compressive strength (MPa)	Maximize	18.35	23.12	++++
Flexural strength (MPa)	Maximize	4.13	5.16	+++
Thermal conductivity $(W \cdot m^{-1} \cdot K^{-1})$	Minimize	0.67	0.70	+++++

why thermal conductivity is more sensitive to slag is that the slag particle is much smaller than FA, which has a "microaggregate effect" that hinders more heat transfer channels and reduces thermal conductivity better. Furthermore, the "pozzolanic effect" caused by slag hydration products can make the mortar more compact and further narrow the heat transfer channel [29] (Table 9).

4.2 Optimum formulation

In this method, the desired value d_i of an individual response is defined in the range of 0–1. In detail, $d_i = 0$ means that the individual response is beyond the acceptable scope, and $d_i = 1$ means that the individual response is at the desired level [30]. With consideration of each desired value d_i , the global desirability function D is defined as follows:

$$D = (d_1 \cdot d_2 \cdot \dots \cdot d_n)^{\frac{1}{n}} = \left(\prod_{i=1}^n d_i\right)^{\frac{1}{n}},$$
 (5)

where D is the global desirability function, d_i is the desirable range for each response, and n is the number of response variables. The importance of an individual response among all responses is marked by the plus symbol (+). By default, all responses are equally important and marked by "+++". If one response is more important, the symbol of "+++" increases to "++++" or "+++++", and *vice versa*.

Due to the low cost of FA and slag originated from industrial and municipal solid waste, the importance degrees of FA and slag are set as "++". More attention

Table 11: Reference group, actual test results, and predicted values

Factors and responses	Mortar	Test results	Predicated values	Error (%)
PO 42.5 (%)	100	56.49	56.49	0
FA (%)	0	20.73	20.73	0
Slag (%)	0	21.49	21.49	0
Fluidity (mm)	115.52	121.15	122.96	1.49
Compressive strength (MPa)	18.28	23.01	23.12	0.48
Flexural strength (MPa)	4.51	4.80	4.83	0.63
Thermal conductivity (W·m ⁻¹ ·K ⁻¹)	0.701	0.66	0.67	1.52

should be paid to compressive strength and thermal conductivity. Thus, compressive strength and thermal conductivity are set to be of "++++" and "+++++" importance levels, respectively. The optimization targets and constraints in this study are listed in Table 10. The goal of mortar optimization is to identify the best case that can meet all the requirements. The optimization was conducted in the "Optimization Part" in Design-Expert version 12.0.6 software. The predicted model gave the optimum combinations among response variables, including fluidity, compressive strength, flexural strength, and thermal conductivity. The comparison between test results and predicted values is performed in Table 11 with reference to GHB mortar. It can be found that the predicted values match well with those in the test, with an error within 1.52%. It is further demonstrated that the model can give an accurate prediction of the optimum contents of GHB mortar.

The results show that both FA and slag are effective in GHB mortar to improve its fluidity, compressive strength, and flexural strength and reduce thermal conductivity. As shown in Table 11, the optimum values of FA and slag are 20.73 and 21.49%, respectively. The global desirability function of the predicted model can reach 0.853, which is higher than 0.706 in the literature [31]. The pore structure of GHB mortar is refined due to the physical filling effect and microaggregate effect of FA and slag. The mortar mixed with FA and slag became more compact, with more heat transfer channels hindered and narrowed, which ultimately made the thermal conductivity drop to 0.67.

5 Conclusions

Based on the RSM, this article explored the influence of the content of FA and slag on the performance of GHB thermal insulation mortar. The performance included fluidity, compressive strength, flexural strength, and thermal conductivity. A multi-objective nonlinear optimization was carried out to identify the optimum contents of FA and slag and ultimately improve the performance of mortar. Some significant conclusions obtained from the statistical analysis and experiment are as follows:

- The RSM is proved to be efficient in revealing and predicting the influence of FA and slag components on the performance of GHB mortar. All the developed regression models for fluidity, compressive strength, flexural strength, and thermal conductivity were demonstrated significantly by the basic evaluation indexes.
- 2) The increase in FA can improve the fluidity of GHB mortar within 30% of its contents, while the effect of

slag can be neglected. The phenomena are associated with the smooth surface of FA particles and the irregular and polygonal surfaces of slag particles, which determine the friction of particles and the fluidity of mortars.

- 3) Both FA and slag have significant effects on compressive strength owing to the physical filler effect. There is a maximum compressive strength at the point of 20% FA and 25% slag. However, the flexural strength is more controlled by the content of FA than slag. There is a negative correlation between the contents of FA and flexural strength due to the "diluting action" of FA.
- 4) The thermal conductivity is significantly influenced by slag. Due to the smaller size of particles, slag and its hydration products perform the microaggregate and pozzolanic effects that hinder more heat transfer channels and reduce thermal conductivity better.
- 5) By maximizing fluidity and compressive and flexural strength and minimizing thermal conductivity, the optimal values of design variables can be obtained as a FA content of 20.73% and a slag content of 21.49%. Compared with the reference group, the performance of GHB mortar can be obviously improved, and all response variables can be well balanced.

Acknowledgments: Authors appreciate the reviewers for their fruitful suggestions to improve the article.

Funding information: This work was supported by the Opening Foundation of Fujian Provincial Applied Technological Engineering Center (LSJZ22-01), the Natural Science Foundation of China (52078079), the Chongqing Technology Innovation and Application Development Special General Project (cstc2020jscx-msxmX0084), the Guangzhou Basic and Applied Basic Research Project (202201010750), the Chongqing Construction Science and Technology Project (Urban S&T 2021 No. 1-8), and the cementious materials reducing admixture for concrete project of GT New Materials and Infrastructure Technology Co., Ltd (Project No. GTRD202001).

Author contributions: Dong Li and Yuhang Pan contributed to the writing and editing. Changjiang Liu contributed to conceptualization, project administration, and funding acquisition. Peiyuan Chen and Yuyou Wu contributed to methodology and writing-reviewing. Jian Liu, Zhoulian Zheng, and Guangyi Ma contributed to supervision and editing.

Conflict of interest: The authors declare that they have no conflict of interest.

Data availability statement: The data used to support the findings of this study are included within the article.

References

- [1] Gu, T. S., L. Y. Xie, and G. Chen. Building energy conservation and wall thermal insulation. *Engineering Mechanics*, Vol. 23, No. 2, 2006, pp. 167–184.
- [2] Othuman, M. A. and Y. C. Wang. Elevated-temperature thermal properties of lightweight foamed concrete. *Construction and Building Materials*, Vol. 25, No. 2, 2011, pp. 705–716.
- [3] Patel, D., R. Shrivastava, R. P. Tiwari, and R. K. Yadav. The role of glass powder in concrete with respect to its engineering performances using two closely different particle sizes. Structural Concrete, Vol. 22, No. 1, 2020, pp. 228–244.
- [4] Shen, Y. N., J. T. Huang, X. B. Ma, F. Hao, and J. F. Lv. Experimental study on the free shrinkage of lightweight polymer concrete incorporating waste rubber powder and ceramsite. *Composite Structures*, Vol. 242, 2020, id. 112152.
- [5] Harith, I. K. Study on polyurethane foamed concrete for use in structural applications. *Case Studies in Construction Materials*, Vol. 8, 2018, pp. 79–86.
- [6] Narayanan, N. and K. Ramamurthy. Structure and properties of aerated concrete: a review. Cement and Concrete Composites, Vol. 22, No. 5, 2000, pp. 321–329.
- [7] Zhang, L. F. and J. J. Zhai. Application of response surface methodology to optimize alkali-activated slag mortar with limestone powder and glass powder. *Structural Concrete*, Vol. 22, No. 1, 2020, pp. 430–441.
- [8] Papadopoulos, A. M. State of the art in thermal insulation materials and aims for future developments. *Energy and Buildings*, Vol. 37, No. 1, 2005, pp. 77–86.
- [9] Tu, J. S., Y. J. Wang, M. Zhou, and Y. Zhang. Heat transfer mechanism of glazed hollow bead insulation concrete. *Journal* of *Building Engineering*, Vol. 40, 2021, id. 102629.
- [10] Xiong, H., K. Yuan, M. Wen, A. Yu, and J. Xu. Influence of pore structure on the moisture transport property of external thermal insulation composite system as studied by NMR. *Construction* and *Building Materials*, Vol. 228, 2019, id. 116815.
- [11] Liu, Y., W. Wang, Y. Zhang, and Z. Li. Mechanical properties of thermal insulation concrete with a high volume of glazed hollow beads. *Magazine of Concrete Research*, Vol. 67, No. 13–14, 2015, pp. 693–706.
- [12] Zhao, L., W. Wang, Z. Li, and Y. F. Chen. An experimental study to evaluate the effects of adding glazed hollow beads on the mechanical properties and thermal conductivity of concrete. *Materials Research Innovations*, Vol. 19, No. 5, 2015, pp. 929–935.
- [13] Wang, J. Y. Analysis of new inorganic exterior insulation materials and thermal energy storage. *Thermal Science*, Vol. 24, No. 5, 2020, pp. 3195–3203.

- [14] Fan, S. J. and P. M. Wang. Effect of fly ash on drying shrinkage of thermal insulation mortar with glazed hollow beads. *Journal* of Wuhan University of Technology, Vol. 32, No. 6, 2017, pp. 1352–1360.
- [15] Zaibo, Z., L. Juanhong, W. Aixiang, and W. Hongjiang. Coupled effects of superplasticizers and glazed hollow beads on the fluidy performance of cemented paste backfill containing alkali-activated slag and MSWI fly ash. *Powder Technology*, Vol. 399, 2022, id. 116726.
- [16] Wan, R., D. Kong, J. Kang, T. Yin, J. Ning, and J. Ma. The experimental study on thermal conductivity of backfill material of ground source heat pump based on iron tailings. *Energy and Buildings*, Vol. 174, 2018, pp. 1–12.
- [17] Ghosh, A., A. Ghosh, and S. Neogi. Reuse of fly ash and bottom ash in mortars with improved thermal conductivity performance for buildings. *Heliyon*, Vol. 4, 2018, id. 00934.
- [18] Wang, W., L. Zhao, Y. Liu, and Z. Li. Mechanical properties and stress-strain relationship in axial compression for concrete with added glazed hollow beads and construction waste. *Construction* and Building Materials, Vol. 71, No. 4, 2014, pp. 425–434.
- [19] He, Z. M. and J. Z. Liu. Influence of fly ash and air entraining agent on performance of thermal insulating mortar blended with vitrified microsphere. *Industrial Construction*, Vol. 40, No. 3, 2010, pp. 102–107.
- [20] Juenger, M. C. and H. M. Jennings. Examining the relationship between the microstructure of calcium silicate hydrate and drying shrinkage of cement pastes. *Cement and Concrete Research*, Vol. 32, No. 2, 2002, pp. 289–296.
- [21] Bashir, M. J. K., H. A. Aziz, M. S. Yusoff, and M. N. Adlan. Application of response surface methodology (RSM) for optimization of ammoniacal nitrogen removal from semi-aerobic landfill leachate using ion exchange resin. *Desalination*, Vol. 254, No. 1–3, 2010, pp. 154–161.
- [22] Ministry of Housing and Urban-Rural Construction of the People's Republic of China. Standard for test method of performance on building mortar. Publication JGJ/T70-2009. China Government Printing Office, Beijing; 2009.

- [23] The State Bureau of Quality and Technical Supervision.

 Method of testing cements-Determination of strength.

 Publication GB/T 17671-2021. China Government Printing

 Office, Beijing; 2021.
- [24] Standardization Administration of China. Test method for effective thermal conductivity of wall materials. Publication GB/T32981-2016. China Government Printing Office, Beijing; 2016.
- [25] Jia, J. Y. and X. L. Gu. Effects of coarse aggregate surface morphology on aggregate-mortar interface strength and mechanical properties of concrete. *Construction and Building Materials*, Vol. 294, 2021, id. 123515.
- [26] Zhu, F., N. Huang, S. Xue, W. Hartley, Y. Li, and Q. Zou. Effects of binding materials on microaggregate size distribution in bauxite residues. *Environmental Science and Pollution Research*, Vol. 23, No. 23, 2016, pp. 23867–23875.
- [27] Khan, M. N., M. Jamil, M. R. Karim, M. F. Zain, and A. B. Kaish. Filler effect of pozzolanic materials on the strength and microstructure development of mortar. KSCE Journal of Civil Engineering, Vol. 21, 2017, pp. 274–284.
- [28] Cao, C., W. Sun, and H. Qin. The analysis on strength and fly ash effect of roller-compacted concrete with high volume fly ash. Cement and Concrete Research, Vol. 30, 2000, pp. 71–75.
- [29] Navrátilová, E. and P. Rovnaníková. Pozzolanic properties of brick powders and their effect on the properties of modified lime mortars. *Construction and Building Materials*, Vol. 120, 2016, pp. 530–539.
- [30] Guo, P., Z. Cao, S. Chen, C. Chen, J. Liu, and J. Meng. Application of Design-Expert response surface methodology for the optimization of recycled asphalt mixture with waste engine oil. *Journal of Materials in Civil Engineering*, Vol. 33, No. 5, 2021, id. 04021075.
- [31] Ma, Z., H. Wang, B. Hui, D. Jelagin, Z. You, and P. Feng. Optimal design of fresh sand fog seal mortar using response surface methodology (RSM): Towards to its workability and rheological properties. *Construction and Building Materials*, Vol. 340, 2022, id. 127638.